

Theory of donor-bound multiexciton complexes in germanium and silicon

Robert S. Pfeiffer

Department of Physics, University of California, San Diego, La Jolla, California 92093

Herbert B. Shore

Department of Physics, San Diego State University, San Diego, California 92182

(Received 5 November 1981)

The energetics of exciton complexes bound to donors in silicon and germanium are investigated using the density-functional method. Two sets of calculations are reported. First, with the use of a simplified model for the semiconductor band structure, energies and densities are calculated for complexes of size M up to about 250 electron-hole pairs. From this, surface and curvature energies and the energy of binding of the complex to the donor are extracted. Second, the energies of the ground and low-lying excited states for small ($M \leq 6$) complexes are calculated, with band-structure effects being taken into account. The results are in good agreement with experimental recombination spectra. Assumptions used in the calculation are critically examined and unanswered theoretical questions discussed.

I. INTRODUCTION

With the discovery of large electron-hole droplets and bound excitons, much interest has developed in the problem of aggregates of intermediate size, such as bound multiexciton complexes (BMEC's) and small droplets. A number of experiments have resulted in detailed line spectra for silicon¹⁻⁴ and germanium⁵⁻⁷ doped with a variety of elements. These lines have been attributed to the recombination of electrons and holes in BMEC's attached to donor or acceptor atoms.

Kirczenow⁸ has proposed a shell model for BMEC's to account for the experimental spectra. In this model, each electron or hole goes into a distinct single-particle orbital, and therefore the electron and the hole which recombine to produce a spectral line can each be assigned to a definite orbital. The electrons and holes do not form exciton-like pairs inside a BMEC. Instead, the shell model treats a BMEC constructed from a neutral donor and M excitons as a system consisting of a central positive charge, M holes, and $M + 1$ electrons, each in independent orbitals.

In this paper we report two methods for calculating the energies of BMEC's; one for large complexes and another, more detailed and accurate, for small complexes. Both methods employ the density-functional theory described in Sec. II and Refs. 9 and 10.

The method we use for large complexes enables

us to calculate the energies of BMEC's of size $M > 200$, and compare the results with calculations and experiments with electron-hole droplets. We compare a variety of properties, such as surface energy, bulk density, and others in Sec. III.

For this simple method, we use an effective-mass approximation to describe the band structure of the host semiconductor, using density-of-states masses for the electrons, the light holes, and the heavy holes, which we treat as three kinds of particles. We have previously published¹¹ the energies of BMEC's in germanium for size $M \leq 10$, and Rose, Sander, and ourselves^{12,13} have discussed the properties of large unbound complexes in germanium. Wünsche *et al.*¹⁴ have also calculated BMEC energies for small complexes using the density-functional method, approximating the band structure with a single optical hole mass and the optical electron mass. In this paper we will present the result of calculations of energies of large BMEC's in both silicon and germanium, compare them with Rose *et al.*'s calculations of the energies of complexes not attached to a donor or acceptor, and compare their properties to those of electron-hole droplets.

Our calculations of the energies of small complexes include details of the semiconductor band structure which have not been included in previous density-functional calculations. In addition, we are able to distinguish between donor elements by means of a central-cell potential. Chang and

McGill¹⁵ have done a configuration-interaction Hartree-Fock calculation that includes band-structure effects, but their calculated ground-state energy for a complex of size M is less negative than the energy of a complex of size $M - 1$ and a free exciton; therefore such a complex would not form. The failure of the Hartree-Fock theory to predict binding indicates that correlation energy plays a critical role in the binding of BMEC's. In our density-functional approach, the correlation energy is of about the same magnitude as a uniform electron-hole gas of equivalent density. The results of our calculations, contained in Sec. V, indicate that BMEC's of all sizes (except for complexes attached to arsenic in silicon) are bound. In addition, the spectra we predict, in the case of all donors in germanium and of phosphorus in silicon, agree well with the actual measured spectra.

The structure of the paper is as follows. In Sec. II we describe density-functional theory as it applies to BMEC's. Section III presents our calculations of the energies of large complexes by means of a simple effective-mass theory. Section IV describes in detail the inclusion of the band-structure effects which are needed for more accurate calculations. Section V gives the energies of small BMEC's as calculated by the method of Sec. IV, and the resulting predicted positions of recombination lines, which it compares with the experimental spectra. Section VI briefly describes several variations of the density-functional method and discusses the results of calculations of BMEC energies by these methods. Section VII concludes with a general discussion of the results, addressing in particular the question of the simultaneous validity of the shell model and of a density-functional theory incorporating a large exchange-correlation energy.

II. THEORY

The density-functional method allows one to solve a many-body problem by solving Schrödinger-type equations for single-particle-like "wave functions" in a self-consistent effective potential. We first review this method as applied to a single type of particle.

Hohenberg and Kohn⁹ showed that for the ground state of a many-body system, the many-body wave function ψ , the external potential $V_{\text{ext}}(\vec{r})$ and the total energy E are functionals of the total density $\rho(\vec{r})$; that is, a given $\rho(\vec{r})$ uniquely determines ψ , $V_{\text{ext}}(\vec{r})$, and E .

Kohn and Sham¹⁰ used this theory to derive

single-particle equations which can be solved for single-particle wave functions. Let the total energy be:

$$E = T + E_{\text{ext}} + E_{\text{Coul}} + E_{\text{xc}} . \quad (1)$$

T is the kinetic energy of the noninteracting electron gas of density $\rho(r)$.

$$E_{\text{ext}} = \int d^3r V_{\text{ext}}(\vec{r})\rho(\vec{r})$$

is the external potential energy, and

$$E_{\text{Coul}} = \int d^3r \int d^3\vec{r}' \frac{1}{2}\rho(\vec{r}) \times \frac{e^2}{|\vec{r} - \vec{r}'|} \rho(\vec{r}') \quad (1')$$

is the electrostatic energy of the system. If $\rho(\vec{r})$ varies slowly one can also use a locally varying functional $\epsilon[\rho(\vec{r})]$ to approximate the exchange-correlation energy, which may include changes in the kinetic energy due to interactions:

$$E_{\text{xc}} = \int d^3r \rho(\vec{r})\epsilon[\rho(\vec{r})] . \quad (1'')$$

Since the ground-state energy is a minimum with respect to all variations of the density that keep the total number of particles fixed, we obtain:

$$\int d^3r \delta\rho(\vec{r}) \left[V_{\text{ext}}(\vec{r}) + \frac{\delta T}{\delta\rho(\vec{r})} + V_{\text{Coul}}(\vec{r}) + \mu_{\text{xc}}(\vec{r}) - \lambda_i \right] = 0 , \quad (2)$$

where

$$V_{\text{Coul}}(\vec{r}) = \int d^3r' \frac{e^2\rho(\vec{r}')}{|\vec{r} - \vec{r}'|} , \quad (2')$$

and

$$\mu_{\text{xc}}(\vec{r}) = \frac{\delta}{\delta\rho(\vec{r})} \{ \rho(\vec{r})E_{\text{xc}}[\rho(\vec{r})] \} . \quad (2'')$$

The functional derivative of the kinetic energy T produces a Schrödinger-type equation with kinetic energy term $-\nabla^2/2m$, eigenvalues λ_i , and effective potential $V(r)$:

$$V(r) = V_{\text{ext}}(\vec{r}) + V_{\text{Coul}}(\vec{r}) + \mu_{\text{xc}}(\vec{r}) . \quad (3)$$

By solving this equation, one obtains single-particle-like wave functions $\psi_i(\vec{r})$, and the total density

$$\rho(r) = \sum_i |\psi_i(\vec{r})|^2 . \quad (4)$$

Equations (2)–(4) form a set of self-consistent

equations for $V(\vec{r})$ and $\rho(\vec{r})$ which one can solve by iteration.

In a BMEC, the total energy E is a functional of both the total electron density $\rho_e(\vec{r})$ and the total hole density $\rho_h(\vec{r})$. By taking derivatives of the energy with respect to both densities, we obtain two separate Schrödinger-type equations, one for electrons and one for holes, each with its own effective potential. One is then able to use single-electron (donor) theory to solve the electron equation and single-hole (acceptor) theory to solve the hole equation. The effective potentials have the following form:

$$\begin{aligned} V_e(\vec{r}) &= -V_{\text{ext}}(\vec{r}) - V_{\text{Coul}}(\vec{r}) + \mu_{xce}(\vec{r}), \\ V_h(\vec{r}) &= V_{\text{ext}}(\vec{r}) + V_{\text{Coul}}(\vec{r}) + \mu_{xch}(\vec{r}). \end{aligned} \quad (5)$$

We deal with the external potential in Sec. IV. Since it is due to electrostatic interaction between the donor atom and the particles, it has opposite signs for electrons and holes. The Coulomb potential has the form:

$$V_{\text{Coul}}(r) = e^2 \int d^3r' \frac{\rho_h(\vec{r}') - \rho_e(\vec{r}')}{|\vec{r} - \vec{r}'|}.$$

We use a simple parametrized local exchange-correlation energy of the form:

$$\epsilon_{xc}[\rho(\vec{r})] = A_e \rho_e^{1/3} + A_h \rho_h^{1/3} + B_e \rho_e^{1/6} + B_h \rho_h^{1/6}. \quad (6)$$

A_e is the coefficient of the exchange energy of a gas of conduction-band electrons and A_h is the coefficient of the exchange energy of a gas of holes. We obtain values of A_e and A_h for both silicon and germanium from Ref. 16. To obtain our expression for the correlation energy (the terms B_e and B_h) we used Rose and Shore's¹⁷ calculation of the correlation energy of a uniform electron-hole gas. Reference 17 expresses the correlation energy as

$$\epsilon(\rho_h, \rho_e) = \epsilon_1(\rho) + \epsilon_2(\rho)(\rho_h - \rho_e), \quad (6')$$

where $\rho = (\rho_e + \rho_h)/2$. The ρ dependence of ϵ_1 and ϵ_2 are such that for almost any value of ρ , one can approximate ϵ as the sum of terms in $\rho_e^{1/6}$ and $\rho_h^{1/6}$. In the case of silicon, we combine Kalia and Vashishta's¹⁸ calculation of the correlation energy of a gas where $\rho_e = \rho_h$ and Rose's¹⁹ calculation of the correlation energy for the case $\rho_h = 0$. This also produces an overall correlation energy of the form indicated by Eq. (6), with specific values for B_e and B_h , valid for densities $\rho_e \geq \rho_h$.

We are able to successfully use a correlation energy of the form of Eq. (6) because the electron and hole densities in BMEC's behave in one of two ways, to both of which Eq. (6) applies, over almost all of the volume occupied by a BMEC:

(1) Near the donor atom, the donor's positive charge repels holes and attracts electrons, leaving the electron density far greater than the hole density. Only electron-electron correlation is then significant, and the $B_e \rho_e^{1/6}$ term adequately describes the correlation energy while the $B_h \rho_h^{1/6}$ term vanishes.

(2) In most of the BMEC's volume, the electron and hole densities are almost equal, and one may arbitrarily distribute the energy between electron and hole terms.

Our form of the correlation energy has the advantage of generating a chemical potential with no negative powers of ρ_e or ρ_h , which is fairly stable under iteration, but includes no explicit correlation between electrons and holes.

If we combine Eqs. (2'') and (6) we obtain the chemical potentials:

$$\mu_{xce}(\vec{r}) = \frac{4}{3} A_e [\rho_e(\vec{r})]^{1/3} + \frac{7}{6} B_e [\rho_e(\vec{r})]^{1/6},$$

$$\mu_{xch}(\vec{r}) = \frac{4}{3} A_h [\rho_h(\vec{r})]^{1/3} + \frac{7}{6} B_h [\rho_h(\vec{r})]^{1/6}.$$

Thus, we are able to include the exchange-correlation energy in an effective potential for single-particle-like wave functions. The existence of two separate equations, one for electrons and one for holes, allow us to exploit techniques which were developed to include details of band structure in calculations of the energies of donor and acceptor states in the calculations of BMEC electron and hole orbitals.

III. PROPERTIES OF LARGE COMPLEXES

We have calculated energies of complexes up to $M = 280$ for silicon and $M = 282$ for germanium by using the density-functional method and simple effective-mass theory. The only feature of band structure we include at this point is the fact that the conduction band of silicon has six equivalent minima and that of germanium has four. Thus, the s , p , and d electron orbitals have degeneracies of 8, 24, and 40, respectively, for germanium; and 12, 36, and 60 for silicon. We use the density-of-states masses of Ref. 16 for all particles, treating light and heavy holes as distinguishable, and use a

TABLE I. Heavy- and light-hole occupation for large complexes.

	M	N_h	N_l	N_h/N_l	$(m_h/m_l)^{3/2}$
Si	260	220	40	5.5	6.24
Ge	282	274	8	34.25	29.56

simple external potential $V_{\text{ext}}(\vec{r})=1/\epsilon r$, where ϵ is the static dielectric constant.

The results for energy and density show several distinct trends as M increases. The orbitals are filled in approximately the same order as they would be in a three-dimensional harmonic oscillator, but the degeneracy of harmonic-oscillator levels is broken, with higher angular-momentum orbitals tending to be occupied first. Thus, silicon at $M=260$ has the configuration: for light holes,

$$1s^2 - 2p^6 - 2s^2 3d^{10} - 3p^6 4f^{14},$$

heavy holes,

$$1s^2 - 2p^6 - 2s^2 3d^{10} - 3p^6 4f^{14} - 5g^{18} 3s^2 4d^{10} \\ - 6h^{22} 5f^{14} 4p^6 - 7i^{26} 6g^{18} 5d^{10} 4s^2 - 8j^{30} 7h^{22},$$

electrons,

$$1s^{12} - 2p^{36} - 2s^{12} 3d^{60} - 4f^{84} 3p^{36} - 5g^{21},$$

and germanium at $M=282$ has the configuration: for light holes,

$$1s^2 - 2p^6,$$

heavy holes,

$$1s^2 - 2p^6 - 2s^2 3d^{10} - 3p^6 4f^{14} - 5g^{18} 3s^2 4d^{10} \\ - 6h^{22} 5f^{14} 4p^6 - 7i^{26} 6g^{18} 5d^{10} 4s^2 \\ - 8j^{30} 7h^{22} (9k^{34}) 5p^6 6f^{14},$$

electrons,

$$1s^8 - 2p^{24} - 2s^8 3d^{40} - 4f^{56} 3p^{24} \\ - 5g^{72} 4d^{40} 3s^8 - 6h^3.$$

We list orbitals in order of increasing energy and separate different harmonic-oscillator levels with dashes. In only one case do harmonic-oscillator levels overlap: In germanium the $9k$ orbital (indicated in parentheses), which belongs to the ninth harmonic-oscillator level, fills before the $5p$ and $6f$ orbitals, which belong to the eighth level.

In a large electron-hole droplet or in an electron-hole liquid, the ratio of heavy to light holes is $N_h/N_l=(m_h/m_l)^{3/2}$, where m_h and m_l are

the heavy- and light-hole masses. The configurations above give numbers of both light and heavy holes; we compare their ratios with the large-droplet ratio in Table I. There is good agreement even for the relatively small complexes considered here. A further comparison between properties of very large droplets and moderately large BMEC's can be obtained by noting that for the electron-hole liquid, it is possible to obtain the energy per pair $\tilde{E}=T+\epsilon_{xc}$ as a function of the density ρ . The kinetic energy is

$$T = \frac{3}{5} \hbar^2 (k_{Fe}^2/2m_e + k_{Fh}^2/2m_h),$$

where k_{Fe} and k_{Fh} are, respectively, the Fermi momenta of electrons and heavy holes. If we express the k_f as functions of the density ρ , we can then obtain the bulk density and energy by minimizing the total energy $\tilde{E}=T+\epsilon_{xc}$ with respect to the density ρ . Thus, $\rho_{\text{bulk}}=2.39 \times 10^{17} \text{ cm}^{-3}$, $\tilde{E}=-6.38 \text{ meV}$ for germanium; and $\rho_{\text{bulk}}=3.37 \times 10^{18} \text{ cm}^{-3}$, $\tilde{E}=-22.01 \text{ meV}$ for silicon.

Figure 1 shows $\rho_h(\vec{r})$ for $M=50, 100$, and 200 . If we define the average density of a BMEC of size M by the relation $(4\pi/3)r^3\rho_m=M$, where $\rho(\vec{r})=\frac{1}{2}\rho_{\text{bulk}}$, we obtain values for ρ_m as follows:

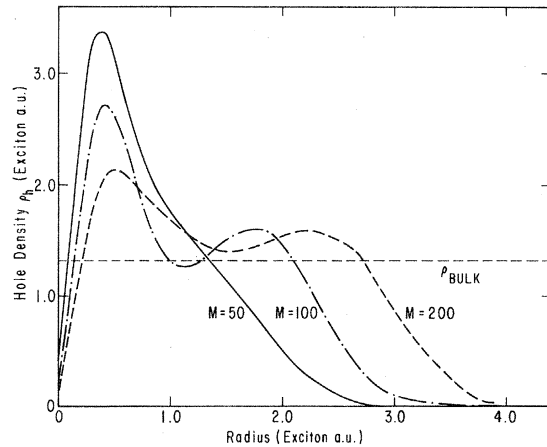


FIG. 1. Hole densities ρ_h as a function of radius for BMEC of sizes $M=50, 100$, and 200 in germanium. The unit of length is 177 \AA .

$\rho_{50}=1.38\rho_{\text{bulk}}$, $\rho_{100}=1.20\rho_{\text{bulk}}$, and $\rho_{200}=1.15\rho_{\text{bulk}}$.

We are also able to obtain surface energies and energies of attachment of droplets to donors which agree with previously calculated bulk values. We suppose that the total energy of a complex $E(M)$ can be fit approximately by an expansion in powers of $M^{1/3}$

$$E(M) \approx \tilde{E}M + BM^{2/3} + CM^{1/3} + D. \quad (7)$$

Here \tilde{E} is the bulk energy per pair obtained above, while B , C , and D are related, respectively, to the surface energy, curvature energy, and energy of attachment of the complex to the bare donor. If one assumes a value for D and defines

$$F(M) = [E(M) - \tilde{E}M - D] / M^{1/3}, \quad (8)$$

then a plot of $F(M)$ vs $M^{1/3}$ should be approximately a straight line with slope B and intercept C . The deviation from a straight line represents the effects of filling of electron and hole shells on the energy.

Figure 2 shows F vs $M^{1/3}$ for BMEC in germanium, using $D = -16.4$ meV. The effects of shell filling are clearly evident. Also shown is a straight-line fit, using values of B and C obtained by a weighted least-squares method. The value of D used in Fig. 2 is chosen to minimize the variance in the straight-line fit to F . The best fit is obtained for $B = 1.34$ meV, $C = 1.31$ meV.

If we define a droplet radius $r(M)$ from

$$M = (4\pi/3)r^3\rho_{\text{bulk}},$$

we can obtain a surface area $S = 4\pi r^2$ and a unit

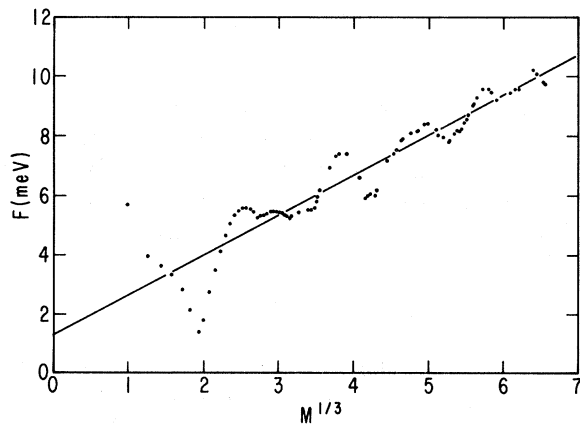


FIG. 2. Least-squares fit of surface and curvature energy of BMEC in germanium. The function $F(M)$ is described in the text and represented by the dots in the figure. The slope and intercept of the linear fit determine the surface and curvature energy, respectively.

of "curvature," $l = 8\pi r$. This enables us to rewrite Eq. (7) as:

$$E = \tilde{E}M + \sigma S + \lambda l + D, \quad (9)$$

and interpret σ as surface tension and λ as curvature energy. For bound complexes in germanium we obtain $\sigma = 1.72 \times 10^{-4}$ ergs/cm², $\lambda = 52.1$ eV/cm. A calculation very similar to the present one has also been performed for *unbound* complexes¹³; i.e., there is no fixed central charge and the number of electrons and holes are equal. The energy $E(M)$ can again be approximated by Eq. (9); in this case we obtain $\sigma = 1.72 \times 10^{-4}$ ergs/cm², $\lambda = 52.5$ eV/cm, $D = 0$. Since the values of σ and λ do not depend on the existence of the donor, we conclude that the σ and λ obtained in this way are in fact characteristic of large drops. Similarly the difference in D with and without the donor corresponds to the binding energy of a large droplet to the central charge.

We can compare our results to other calculations of these quantities. To our knowledge there are no other reported calculations of λ . Sander *et al.*²⁰ calculated -16 meV for the energy of attachment of a large droplet to a donor, in good agreement with our result for D . There are several extant estimates of σ , including theoretical values of 1.98×10^{-4} ergs/cm² by Rose and Shore,¹⁷ 3.7×10^{-4} ergs/cm² by Kalia and Vashishta,¹⁸ and experimental values of $\sim 1 \times 10^{-4}$ ergs/cm² (Ref. 21) and 1.6×10^{-4} ergs/cm².²²

In Fig. 3, we repeat the procedure described above for BMEC in silicon. The minimum variance is obtained for $D = -54.5$ meV, $B = 9.86$ meV, $C = 6.12$ meV. This corresponds to calculated values of $\sigma = 43.7 \times 10^{-4}$ ergs/cm², $\lambda = 588$ eV/cm. This compares with a theoretical value of

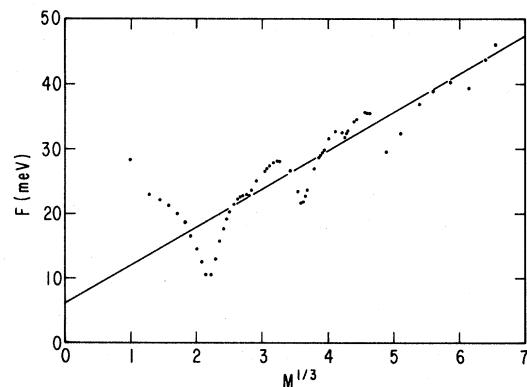


FIG. 3. Least-squares fit of surface and curvature energy of BMEC in silicon. The data are calculated values of $F(M)$.

$\sigma = 87.5 \times 10^{-4}$ ergs/cm² (Ref. 17) and an experimental value of $\sigma = (125 \pm 60) \times 10^{-4}$ ergs/cm².²³ Thus, by using a simple effective-mass theory, we are able to calculate the energies of complexes of size $M > 200$, and these complexes are in turn large enough to closely approximate the energy per electron-hole pair, the density, the ratio of light to heavy holes, the surface tension, and the energy of attachment to a donor of large electron-hole droplets.

IV. THEORY INCORPORATING REALISTIC BAND STRUCTURE

In the previous section we were able to calculate trends in the energy and density for fairly large complexes. The specific details concerning the filling of individual shells were not produced correctly, since we did not incorporate properly any details of the band structure other than the degeneracy of the electron and hole bands. In order to determine ground- and excited-state energies which are sufficiently accurate to enable comparison with detailed spectroscopic data for small ($M \leq 6$) complexes, we make use of methods originally designed for calculating donor and acceptor energies,²⁴⁻²⁷ which we describe in detail in this section. We have already reported the results of calculations which include band-structure effect^{28,29} but used methods for the conduction band which differ in detail from those described below.

Observed energies of BMEC depend on the specific donor element. We incorporate this dependence by introducing an impurity potential which includes an empirical "central-cell" correction:

$$V_{\text{ext}}(\vec{r}) = \frac{e^2}{\epsilon r} (1 + V_0 e^{-r/r_0}). \quad (10)$$

We adjust the central-cell parameters, r_0 (range), and V_0 (strength) to reproduce the experimental values of the donor ground state and lowest excited state.

A. Conduction band

The conduction bands of silicon and germanium have N equivalent minima, called valleys or pockets, which, if there were no coupling between electrons in different valleys, would allow $2N$ degenerate $1s$ states ($N = 4$ for germanium and $N = 6$ for silicon). In fact, coupling between electrons in different valleys splits the $2N$ degeneracy of the $1s$ states. A state of a given energy will be a linear combination of single-valley states possessing a

specific overall cubic group symmetry, while states with different cubic symmetries will have different energies. For example, the donor ground state has cubic symmetry Γ_1 and an amplitude of $\sqrt{1/N}$ for each valley.

Our method for deriving a radial differential equation for the conduction-band wave function is based on, though not identical with, the modified effective-mass theory of Resca and Resta.²⁴ It is based on a modification to the method of Ref. 24 suggested by Resca, Resta, and Shore.²⁵ We describe our version of this method below.

One can represent the pseudo-Bloch wave of an electron at the i th minimum by:

$$\phi(\vec{K}_i, \vec{r}) = e^{i\vec{K}_i \cdot \vec{r}} \sum_{\vec{G}} a_i \vec{G} e^{i\vec{G} \cdot \vec{r}}, \quad (11)$$

where the \vec{G} are reciprocal-lattice vectors. It is then possible to construct an approximate single-electron wave function with group symmetry Γ with the following form:

$$\psi^\Gamma(\vec{r}) = \left[\sum_{i=1}^N \alpha_i^\Gamma \phi(\vec{K}_i, \vec{r}) \right] f^\Gamma(\vec{r}). \quad (12)$$

The α_i^Γ are constants that depend on the representation index Γ . We have assumed that $f^\Gamma(\vec{r})$ has mostly small k components, that $f^\Gamma(\vec{r})$ is the same in all valleys, and that the periodic part of $\phi(\vec{k}, \vec{r})$ is the same as the periodic part of $\phi(\vec{K}_i, \vec{r})$ for \vec{k} near \vec{K}_i .

We seek to derive an equation which we can solve for $f^\Gamma(\vec{r})$, and begin with a representation of ψ^Γ in \vec{k} space, expanding \vec{k} as $\vec{k} = \vec{G} + \vec{K}_i + \vec{\eta}$. Then

$$\psi^\Gamma(\vec{K}_i, \vec{G}, \vec{\eta}) = \alpha_i^\Gamma a_i \vec{G} F^\Gamma(\vec{\eta}), \quad (13)$$

the various vectors $\vec{G} + \vec{K}_i + \vec{\eta}$, constructed from the reciprocal-lattice vectors \vec{G} , the N pocket vectors \vec{K}_i , and $\vec{\eta}$, will cover \vec{k} space precisely if $\vec{\eta}$ is allowed to range over a region covering exactly $1/N$ of the Brillouin zone. Then, and only then will

$$\delta(\vec{k} - \vec{k}') = \delta_{\vec{G}, \vec{G}'} \delta_{ij} \delta(\vec{\eta} - \vec{\eta}').$$

The \vec{k} -space Hamiltonian of a conduction-band electron in a local external potential is as follows:

$$\mathcal{H} = \epsilon(\vec{k}) \delta(\vec{k} - \vec{k}') + V(\vec{k} - \vec{k}'). \quad (14)$$

We take the expectation value with respect to $\psi^\Gamma(\vec{k})$ and $\psi^\Gamma(\vec{k}')$ and subtract the energy, obtaining

$$\int d^3\eta \int d^3\eta' \sum_{i,j=1}^N \alpha_i^{\Gamma*} \alpha_j^{\Gamma} \sum_{\vec{G}, \vec{G}'} a_i^* a_j \{ F^{\Gamma*}(\vec{\eta}) [\epsilon(\vec{\eta} + \vec{k}_i) - E] \delta_{ij} \delta_{\vec{G}, \vec{G}'} \delta(\vec{\eta} - \vec{\eta}') F^{\Gamma}(\vec{\eta}') + V(\vec{\eta} - \vec{\eta}' + \vec{G} + \vec{K}_i - \vec{G}' - \vec{K}_j) F^{\Gamma*}(\vec{\eta}) F^{\Gamma}(\vec{\eta}') \} = 0. \quad (15)$$

If one expands the spherical average of $\epsilon(\vec{K}_i + \vec{\eta})$ around \vec{K}_i one obtains

$$\epsilon(\vec{K}_i + \vec{\eta}) = \epsilon(\vec{K}_i) + (\hbar^2/2m^*)\eta^2.$$

Substituting this expression for the energy in Eq. (15) and integrating, we obtain an equation for $F^{\Gamma}(\vec{\eta})$:

$$\frac{\hbar^2\eta^2}{2m^*} F^{\Gamma}(\vec{\eta}) + \sum_{i,j=1}^N \alpha_i^{\Gamma*} \alpha_j^{\Gamma} \sum_{\vec{G}, \vec{G}'} a_i^* a_j \int_{1/N \text{ zone}} V(\vec{\eta} - \vec{\eta}' + \vec{G} + \vec{K}_i - \vec{G}' - \vec{K}_j) F^{\Gamma}(\vec{\eta}') d^3\eta' = E F^{\Gamma}(\vec{\eta}). \quad (16)$$

In \vec{r} space this equation becomes

$$\frac{-\hbar^2}{2m^*} \nabla^2 f^{\Gamma}(\vec{r}) + V^{\Gamma}(\vec{r}) f^{\Gamma}(\vec{r}) = E f^{\Gamma}(\vec{r}), \quad (17)$$

where

$$V^{\Gamma}(\vec{r}) = \frac{1}{(2\pi)^3} \sum_{\vec{H}} a_{\vec{H}}^{\Gamma} \int_{1/N \text{ zone}} d^3\eta \times V(\vec{\eta} + \vec{H}) e^{i\vec{\eta} \cdot \vec{r}}.$$

Here

$$\vec{H} = \vec{G} + \vec{K}_i - \vec{G}' - \vec{K}_j$$

and

$$a_{\vec{H}}^{\Gamma} = \alpha_i^{\Gamma*} \alpha_j^{\Gamma} a_i^* a_j.$$

In practice we replace the $1/N$ zone integral by a weighted integral over all $\vec{\eta}$ space and spherically average in \vec{r} space, to obtain the radial equation:

$$\frac{-\hbar^2}{2m^*} \nabla^2 f(r) + \tilde{V}^{\Gamma}(r) f(r) = E f(r), \quad (18)$$

where

$$\tilde{V}^{\Gamma}(r) = \int \frac{d\Omega_r}{4\pi} \sum_{\vec{H}} a_{\vec{H}}^{\Gamma} \int_{\text{all space}} d^3\eta \frac{\alpha^4}{(\alpha^2 + \eta^2)^2} \times \frac{1}{(2\pi)^3} V(\vec{\eta} + \vec{H}) e^{i\vec{\eta} \cdot \vec{r}}.$$

The factor $\alpha^4/(\alpha^2 + \eta^2)^2$ is a cutoff factor which limits the integration over $\vec{\eta}$ to the region $\eta \leq \alpha$. The constant α is chosen so that

$$\int d^3\eta \alpha^4/(\alpha^2 + \eta^2)^2 = Z/N,$$

where Z is the volume of the Brillouin zone. This condition is satisfied if

$$\alpha = \frac{2}{a} \left[\frac{4\pi}{N} \right]^{1/3},$$

where a is the lattice constant.

It is useful to give a qualitative description of the meaning of the potential $\tilde{V}^{\Gamma}(r)$. First the original potential $V(r)$ is multiplied by the appropriate symmetry combination of pseudo-Bloch states. The product contains high \vec{k} components, arising from the short-range central-cell part of $V(r)$ and from the high \vec{G} components of the Bloch waves. There are also low \vec{k} components resulting from *mixing* of the high \vec{k} terms in the product. The effect of cutting off the integral over $\vec{\eta}$ is to "filter out" the high \vec{k} terms and leave a $\tilde{V}^{\Gamma}(r)$ that is relatively slowly varying. Since $\tilde{V}^{\Gamma}(r)$ has no high k components, the solution of Eq. (18) will result in an $f(r)$ whose Fourier transform is likewise restricted to the vicinity of a single-valley minimum. As a consequence, the wave function $\psi^{\Gamma}(r)$ contains components from only the lowest conduction band, as was assumed in writing Eq. (13). For a strong central-cell potential, the restriction of ψ^{Γ} to a single band will incorrectly inhibit the collapse of the wave function and the formation of deep states. However, if the restriction were not present, the overlap of k components of the $f(r)$ from different pockets could lead to an artificially enhanced binding energy, and the prediction of deep states for weak central-cell potentials. For the present problem, where we are concerned only with shallow states, the restriction is technically correct but not in fact important. The results reported in this paper, with the restriction on the η integration included, are essentially identical with our earlier work, where the original method of Resta and Resca²⁴ was used; the primary difference

between the two sets of calculations is that different central-cell parameters must be used in order to fit the donor levels.

In practice, the treatment of the potential described above is not applied to the complete self-consistent potential, but only to the impurity potential $V_{\text{ext}}(r)$, since this is the only part of the potential that varies rapidly. Thus, we "process" the impurity potential from Eq. (10) to produce an effective external potential $\tilde{V}^\Gamma(r)$. The radial equation then has the form

$$\frac{-\hbar^2}{2m^*} \nabla^2 f(r) + U^\Gamma(r) f(r) = E f(r), \quad (19)$$

where

$$U^\Gamma(r) = \tilde{V}^\Gamma(r) + V_{\text{Coul}}(r) + \mu_{\text{xce}}(r).$$

Since $\tilde{V}^\Gamma(r)$, and hence $U^\Gamma(r)$, depend on Γ , we have a different effective potential for each cubic symmetry. This allows us to reproduce the splitting of donor levels by adjusting the central-cell parameters r_0 and V_0 . We can then easily solve Eq. (19) using standard numerical methods.

We obtain a ground state with Γ_1 symmetry, and an excited state with Γ_5 symmetry. All these states have 1s radial orbitals.

B. Valence band

The valence bands of germanium and silicon are divided into light, heavy, and split-off bands by interaction between the spin ($s = \frac{1}{2}$) of the holes and the orbital angular momentum ($L = 1$) of the valence band. This produces a spin- $\frac{3}{2}$ band and a split-off spin- $\frac{1}{2}$ band. Away from the center of the Brillouin zone, the asymmetry of the Bloch states splits the spin- $\frac{3}{2}$ band into light- and heavy-hole bands. A nonperiodic potential couples the light and heavy bands, and it is necessary to include this effect to obtain reasonably accurate wave functions and energies for holes in BMEC's.

We use a spherically symmetric approximation, introduced by Baldereschi and Lipari²⁶ for the kinetic-energy term of the acceptor Hamiltonian, to calculate single-particle hole wave functions. The significant factors which this approximation ignores are: (1) the anisotropy of the light- and heavy-hole bands, and (2) coupling with the split-off band. Silicon has a gap of only 44 meV between the spin- $\frac{3}{2}$ and split-off bands and is also highly anisotropic, while germanium has a more spherical valence band and a gap of 290 meV between the spin- $\frac{3}{2}$ and split-off bands; so that one expects the spherical approximation to produce

more accurate acceptor energies in germanium than in silicon. Indeed, Ref. 26 reports acceptor ground-state energies of -31.6 meV for silicon and -9.8 meV for germanium, compared with experimental values of -68.9 meV for aluminum in silicon³⁰ and -10.8 meV for gallium in germanium.³¹

Since the holes in a donor-bound BMEC are repelled from the central donor atom, and bound primarily by correlation energy, their binding energies are small compared to the binding energy of holes attached to acceptors, being on the order of only a few meV. Thus coupling to the split-off band will be weak even in silicon, and the spherical approximation should be more accurate for holes in BMEC's than it is for acceptors.

The spherical Hamiltonian treats a hole in the spin- $\frac{3}{2}$ band as a simple $J = \frac{3}{2}$ particle whose spin couples with the angular momentum of the acceptor (or BMEC hole) orbitals. It has the following form²⁶:

$$\mathcal{H} = -\frac{\hbar^2 \gamma}{2m_0} [(1 + 5\mu/4) \nabla^2 - \mu(\vec{J} \cdot \vec{\nabla})^2] + V(r), \quad (20)$$

where m_0 is the free-electron mass. We choose γ and μ to reproduce the light- and heavy-hole masses. This requires a γ and μ such that $m_l/m_0 = \gamma(1 + \mu)$ and $m_h/m_0 = \gamma(1 - \mu)$, where m_l and m_h are the density-of-states effective masses of light and heavy holes, respectively. This choice of γ and μ differs somewhat from that of Ref. 26, in that it does not correspond to a strict separation of the spherical and cubic terms in the acceptor Hamiltonian; however, by fitting our spherically symmetric hole bands to density-of-states masses, we ensure that the properties of large complexes, i.e., electron-hole droplets, will be reproduced correctly.

The Hamiltonian of Eq. (20) has the following properties. First, $F = |\vec{L} + \vec{J}|$ and F_z are good quantum numbers. Second, it couples orbitals of angular momentum L with those of angular momentum $L + 2$, but not to any other orbitals. This enables one to construct a wave function $\psi(r, \theta, \phi, J_z)$ from radial functions $u(r)$ and $w(r)$ as follows:

$$r\psi(r, \theta, \phi, J_z) = u(r) |L, F, F_z\rangle + w(r) |L + 2, F, F_z\rangle. \quad (21)$$

For example, the ground state has $F = \frac{3}{2}$, $L = 0$, and its $F_z = +\frac{3}{2}$ component has the form

$$r\psi(r, \theta, \phi, J_z) = u(r)[Y_{00}(\theta, \phi) |J_z = \frac{3}{2}\rangle] + w(r)[\sqrt{1/5}Y_{20}(\theta, \phi) |J_z = \frac{3}{2}\rangle - \sqrt{2/5}Y_{2,+1}(\theta, \phi) |J_z = \frac{1}{2}\rangle + \sqrt{2/5}Y_{2,+2}(\theta, \phi) |J_z = -\frac{1}{2}\rangle]. \quad (22)$$

For a given F and L one solves a radial 2×2 matrix equation for $u(r)$ and $w(r)$:

$$\frac{-\hbar^2\gamma}{2m_0} \Omega \begin{pmatrix} u(r) \\ w(r) \end{pmatrix} + V(r) \begin{pmatrix} u(r) \\ w(r) \end{pmatrix} = E \begin{pmatrix} u(r) \\ w(r) \end{pmatrix}, \quad (23a)$$

where the matrix Ω is

$$\Omega = \begin{pmatrix} (1+g\mu) \left[\frac{d^2}{dr^2} - \frac{L(L+1)}{r^2} \right] & -\mu(1-g^2)^{1/2} \left[\frac{d^2}{dr^2} + \frac{2L+3}{r} \frac{d}{dr} + \frac{L(L+2)}{r^2} \right] \\ \mu(1-g^2)^{1/2} \left[\frac{d^2}{dr^2} - \frac{2L+3}{r} \frac{d}{dr} + \frac{(L+1)(L+3)}{r^2} \right] & (1-g\mu) \left[\frac{d^2}{dr^2} - \frac{(L+2)(L+3)}{r^2} \right] \end{pmatrix}. \quad (23b)$$

Here, $g = L/(2L+3)$, when $F = L + \frac{3}{2}$, and $g = -(L+3)/(2L+3)$, when $F = L + \frac{1}{2}$. In addition, there are two one-component states with $F = \frac{1}{2}$. One state has $L = 1$ and the other $L = 2$. They are solutions of the radial equation

$$\frac{-\hbar^2\gamma}{2m_0} (1+\mu) \left[\frac{d^2}{dr^2} - \frac{L(L+1)}{r^2} \right] rf(r) + V(r)rf(r) = Erf(r). \quad (23c)$$

We solve Eq. (23a) for $u(r)$ and $w(r)$ numerically by using a modification of a method developed by Mendelson and James²⁷ for finding the ground and lower excited states of acceptors. One begins by finding series solutions to Eq. (23a). The equation has two series solutions. One has the form:

$$u_1(r) = \sum_{k=0}^{\infty} a_k r^{k+L+3}, \quad (24a)$$

$$w_1(r) = \sum_{k=0}^{\infty} b_k r^{k+L+3}.$$

Each series resembles the expansion of a single-component wave function of angular momentum $L+2$, multiplied by r . The second series has the form:

$$u_2 = \sum_{k=0}^{\infty} c_k r^{k+L+1} + \alpha u_1(r) \ln r, \quad (24b)$$

$$w_2(r) = \sum_{k=1}^{\infty} d_k r^{k+L+1} + \alpha w_1(r) \ln r.$$

The polynomial terms of these series have the same

form as the series of a wave function of angular momentum L multiplied by r . If one substitutes the series $[u_2(r), w_2(r)]$ into Eq. (23a), one obtains two equations for the three unknowns c_2 , d_2 , and α . One equation determines α , and the other relates c_2 and d_2 . Thus, c_2 is undetermined and we can assign it an arbitrary value, which in our calculations is $c_2 = 0$. Changing c_2 is equivalent to replacing $[u_2(r), w_2(r)]$ by $[u_2(r), w_2(r)] + \beta[u_1(r), w_1(r)]$.

We extend $[u_1(r), w_1(r)]$ and $[u_2(r), w_2(r)]$ out to large distances by integrating Eq. (23a) via the Runge-Kutta method. If E is not an eigenvalue then all linear combinations of $[u_1(r), w_1(r)]$ and $[u_2(r), w_2(r)]$ will diverge, while at an energy which is an eigenvalue of Eq. (23a), some linear combination of $[u_1(r), w_1(r)]$ and $[u_2(r), w_2(r)]$ will converge to zero as $r \rightarrow \infty$. At large radius, solutions of Eq. (23a) would have one of two forms:

$$\begin{pmatrix} u_-(r) \\ w_-(r) \end{pmatrix} = \begin{pmatrix} \sqrt{1-g} \\ \sqrt{1+g} \end{pmatrix} e^{-K_- r}, \quad K_-^2 = \frac{-2m_0 E}{\hbar^2 \gamma (1-\mu)}, \quad (25a)$$

$$\begin{pmatrix} u_+(r) \\ w_+(r) \end{pmatrix} = \begin{pmatrix} \sqrt{1+g} \\ \sqrt{1-g} \end{pmatrix} e^{-K_+ r}, \quad K_+^2 = \frac{-2m_0 E}{\hbar^2 \gamma (1+\mu)}. \quad (25b)$$

Extending $[u_1(r), w_1(r)]$ will produce $[u_-(r), w_-(r)]$ states at the proper energies. Since the $[u_1(r), w_1(r)]$ are $L+2$ -like series's, which are cou-

TABLE II. Values of the parameters r_0 and V_0 in the impurity potential Eq. (10).

System	r_0 (Å)	V_0
P,Bi:Ge	2.0	12.5
As:Ge	1.8	15.4
P:Si	0.9	35.4
As:Si	0.7	55.4
Sb:Si	0.9	33.0

pled to L states by Eq. (23a), on would expect their energies to be greater than that of the uncoupled (i.e., $\mu=0$) $L+2$ state. Thus, the most bound $[u_-(r), w_-(r)]$ state is less bound than an uncoupled $L=2$ state. Similarly, the one-component wave functions ($F=\frac{1}{2}$) are less bound by a factor of $1/(1+\mu)$ than the corresponding states for $\mu=0$. Thus, the lowest energy of a one-component state is greater than that of an uncoupled $L=1$

state. On the other hand, the $[u_+(r), w_+(r)]$ states, produced by extending $[u_2(r), w_2(r)] + \beta[u_1(r), w_1(r)]$, are more bound than the corresponding states of angular momentum L . Thus, the $|L=0, F=\frac{3}{2}\rangle$, $|L=1, F=\frac{3}{2}\rangle$, and

$$|L=1, F=\frac{5}{2}\rangle[u_+(r), w_+(r)]$$

states are all more bound than an uncoupled $L=1$ state, which, in turn, is more bound than any one-component or $[u_-(r), w_-(r)]$ state. The conclusion is that one can use holes from $[u_+(r), w_+(r)]$ orbitals exclusively to construct BMEC's of size up to $M=14$. Since we calculate energies only up to the $M=6$ ground state, we use only $[u_+(r), w_+(r)]$ hole orbitals.

In sum, we use a spherically symmetric Hamiltonian to obtain two-component radial wave functions by solving Eq. (23a). All our wave functions have the form indicated by Eq. (25b). The ground

TABLE III. Theoretical energies E_M for BMEC in silicon, for $M \leq 6$, for several electron and hole configurations. The energy E_M is taken relative to the energy of a bare donor, M free holes, and $M+1$ free electrons.

M	Electron configuration			Hole configuration		P	$-E_M$ (meV)	
	Γ_1	Γ_5	Γ_3	Γ_8^+	Γ_8^-		donor element	As
0	1	0	0	0	0	45.31	42.58	53.30
	0	1	0	0	0	33.61	32.77	32.47
	0	0	1	0	0	31.37	30.83	29.97
1	2	0	0	1	0	65.13	61.76	72.66
	1	1	0	1	0	58.31	56.02	61.34
	1	0	1	1	0	57.30	55.12	
	2	0	0	0	1	63.40	60.02	73.05
2	2	1	0	2	0	81.45	78.01	83.94
	1	2	0	2	0	75.23	73.05	73.36
	2	0	1	2	0	80.70		
3	2	2	0	3	0	100.61	97.75	101.65
	1	3	0	3	0	95.16	93.11	90.85
4	2	3	0	4	0	122.07	119.68	120.17
	1	4	0	4	0	117.16	115.35	107.25
	2	3	0	3	1	118.53	115.81	118.48
	1	4	0	3	1	113.69	112.05	107.23
5	2	4	0	4	1	142.15	139.69	137.38
	1	5	0	4	1	137.96	136.06	129.08
	2	4	0	3	2	138.51	136.06	135.98
	1	5	0	3	2	134.31	132.04	126.87
6	2	5	0	4	2	163.64	116.15	157.59

state has $L=0$, $F=\frac{3}{2}$ (cubic symmetry Γ_8^+) and the lower excited state has $L=1$, $F=\frac{3}{2}$ (cubic symmetry Γ_8^-).

V. ENERGIES OF SMALL COMPLEXES

When we calculate the energies of BMEC's by the density-functional method and include the band-structure corrections described in Sec. IV, we are able to predict positions of recombination lines which are close to the experimental positions.

We have obtained ground-state energies for complexes up to size $M=6$, and also lowest electron- and hole-excited states for many of the smaller complexes. The elements covered were phosphorus, arsenic, and antimony in silicon; and phosphorus, arsenic, and bismuth in germanium. We chose r_0 and V_0 , the central-cell parameters, to

reproduce the experimental energies of the $\Gamma_1 1s$ and $\Gamma_2 1s$ donor states^{32,33} and obtained the values listed in Table II. Since the central-cell parameters of phosphorus and bismuth in germanium are identical, the BMEC energies will also be the same for both elements. The experimental donor level of antimony in germanium could not be reproduced by our external potential.

The radius r_0 and strength V_0 of our central-cell correction have the same order of magnitude as that obtained by Vinsome and Richardson³⁴ from a study of the q -dependent dielectric function.

We have listed energies of complexes of size up to $M=6$ in Table III for silicon and Table IV for germanium. It is possible to obtain several series of lines from the tables. The most prominent series is the α series, which has been measured up to α_6 in silicon¹ and α_2 in germanium.⁶ An α_M line results from the recombination of a Γ_1 elec-

TABLE IV. Theoretical energies E_M for BMEC in germanium, for $M \leq 6$.

M	Electron configuration		Hole configuration		$-E_M$ (meV) donor element	
	Γ_1	Γ_5	Γ_8^+	Γ_8^-	P,Bi	As
0	1	0	0	0	12.74	14.00
	0	1	0	0	9.74	9.79
1	2	0	1	0	18.44	19.98
	1	1	1	0	16.82	17.78
	2	0	0	1	17.97	19.53
	1	1	0	1	16.48	17.50
2	2	1	2	0	23.14	24.53
	1	2	2	0	21.77	22.60
	2	1	1	1	22.55	23.92
	1	2	1	1	21.27	22.12
3	2	2	3	0	28.67	29.96
	1	3	3	0	27.47	28.16
	2	2	2	1	28.03	29.26
	1	3	2	1	26.87	27.60
4	2	3	4	0	34.90	36.05
	1	4	4	0	33.78	34.39
	2	3	3	1	34.20	35.30
	1	4	3	1	33.07	33.73
5	2	4	4	1	40.93	41.99
	1	5	4	1	39.91	40.45
	2	4	3	2	40.19	41.20
	1	5	3	2	39.22	39.79
6	2	5	4	2	47.40	48.35

tron and a Γ_8^+ hole from the ground state of a complex. The final state has an electron excited if $M > 1$ and an electron and a hole excited if $M > 4$. The β_M series, which has been found up to $\beta_5^{1,2}$ in silicon, and not at all in germanium, results from the recombination of a Γ_5 electron and a Γ_8^+ hole from the ground state of a BMEC of size $M + 1$. It is a ground-to-ground transition if $M < 4$. There are also α' and β' series's, which have been reported in silicon.² They differ from the corresponding α and β series in that the electron combines with a Γ_8^- hole instead of a Γ_8^+ hole. The β' series is the ground-to-ground transition if $M > 3$. In addition, the following transitions in germanium have been reported:

$$\delta: M = 1 (\Gamma_1\Gamma_5, \Gamma_8^+) \rightarrow \text{donor}(\Gamma_1),$$

$$\gamma_1: M = 1 (\Gamma_1\Gamma_5, \Gamma_8^+) \rightarrow \text{donor}(\Gamma_5),$$

$$\epsilon: M = 1 (2\Gamma_1, \Gamma_8^-) \rightarrow \text{donor}(\Gamma_1),$$

$$\alpha_1\Gamma_5: M = 1 (2\Gamma_1, \Gamma_8^+) \rightarrow \text{donor}(\Gamma_5),$$

where the $\alpha_1\Gamma_5$ line, in addition to the recombination of a Γ_1 electron and a Γ_8^+ hole, requires the promotion of a Γ_1 electron to the Γ_5 level, and is therefore forbidden in the shell model.

The calculated energies E_M in Tables III and IV are with respect to the energy of a bare donor, $M + 1$ free electrons, and M free holes. The total energy of a BMEC of size M is $E_{\text{tot}}(M) = M \times E_{\text{gap}} + E_M$, where the gap energy E_{gap} is the energy needed to create an electron-hole pair and has the value of 1169.30 meV for silicon and 744.64 meV

for germanium. The observed photon energy due to recombination of an electron-hole pair is then:

$$\begin{aligned} E_\gamma &= E_{\text{tot}}(M) - E_{\text{tot}}(M - 1) \\ &= E_{\text{gap}} + E_M - E_{M-1}. \end{aligned} \quad (26)$$

For example, for phosphorus in silicon, and α_1 line, which corresponds to the transition

$$M = 1 (2\Gamma_1, \Gamma_8^+) \rightarrow \text{donor}(\Gamma_1),$$

should appear at the position:

$$\begin{aligned} E(\alpha_1) &= E_{\text{gap}} + E_{2\Gamma_1, \Gamma_8^+} - E_{\Gamma_1} \\ &= 1169.30 \text{ meV} \\ &\quad + (-65.13 \text{ meV}) - (-45.13 \text{ meV}) \\ &= 1149.48 \text{ meV}. \end{aligned}$$

This is close to the experimental position of $\alpha_1 = 1150.01$ meV. Table V gives the predicted positions of recombination lines for different donor elements in silicon, with the measured positions in parentheses, while Table VI does the same for germanium. All the predicted positions of BMEC recombination lines in germanium were within 1 meV of their measured values, and the predicted positions of lines in the α series for phosphorus in silicon were also within 1 meV of the measured position.

Our predicted positions of β -series lines (which have been measured experimentally only in silicon) are consistently too near the gap energy, deviating

TABLE V. Theoretical and experimental positions (in meV) of recombination lines for several donor species in silicon. Experimental values are in parentheses; the superscripts refer to the table of references.

Donor :	P	Sb	As
α_1	1149.48 (1150.01) ²	1150.12 (1150.1) ⁵	1149.94 (1149.2) ⁵
α_2	1146.16 (1146.47) ²	1147.31 (1146.7) ⁵	1146.70 (1145.7) ⁵
α_3	1143.92 (1143.71) ²	1144.60 (1144.0) ⁵	1140.99 (1142.5) ⁵
α_4	1142.39 (1141.72) ²	1142.73 (1142.0) ⁵	1139.98 (1140.0) ⁵
α_5	1140.84 (1140.46) ²	1141.66 (1140.50) ⁵	1139.15 (1138.8) ⁵
α_6	1139.97 (1139.31) ²	1140.19	1138.58 (1137.5) ⁵
α_5'	1144.31 (1142.43) ³	1144.96	1139.17
α_6'	1143.62 (1141.27) ³	1144.21	1140.79
β_1	1152.98 (1150.6) ³	1153.05	1158.02 (1151.4) ⁵
β_2	1150.14 (1147.90) ²	1149.56 (1147.4) ⁵	1151.58 (1146.3) ⁵
β_3	1147.84 (1145.60) ²	1147.37 (1145.1) ⁵	1150.78 (1144.6) ⁵
β_4	1145.68 (1144.07) ³	1145.42	1150.40 (1142.9) ⁵
β_5	1144.17 (1143.27) ³	1144.21	1147.69
β_4'	1149.22	1149.29	1152.09
β_5'	1147.77 (1144.79) ³	1147.86	1149.09

TABLE VI. Theoretical and experimental positions (in meV) of recombination lines for several donor species in germanium. Some experimental lines are split into four components. Energies marked by an asterisk were not actually observed, but are deduced from other experimental line positions.

		Donor :	P	Bi	As
α_1	Theor.		738.94	738.94	738.66
	Expt. ⁶		739.21	739.25	739.07
α_2	Theor.		738.32	738.32	737.89
	Expt. ⁶		738.18		737.92
			738.34*		738.12*
			738.48*		738.33
			738.64		738.46
γ_1	Theor.		737.61	737.61	736.63
	Expt. ⁶		737.85		736.70
			737.71		736.50*
			737.56		736.31
			737.41		736.19
δ	Theor.		740.56	740.56	740.86
	Expt. ⁶		740.66	740.70	740.93
			740.54*	740.55*	740.73*
			740.40	740.41	740.54*
			740.24	740.25	740.42
ϵ	Theor.		739.41	739.41	739.21
	Expt. ⁷		740.03	740.03	739.97
$\alpha_1\Gamma_5$	Theor.		735.99	735.99	734.45
	Expt. ⁶		736.41		734.86

from the experimental values by at least 2 meV, and, in the case of arsenic in silicon, by over 6 meV. This is the result of our calculation's overes-

imation of the electron excitation energy. For a complex of size M , this energy (Δ_M) would be equal to $\beta_M - \alpha_{M+1}$. Thus,

$$\begin{aligned} \Delta_1 &= \beta_1 - \alpha_2 = [E_{\text{gap}} + E(2\Gamma_1, \Gamma_5, \Gamma_8^+) - E(2\Gamma_1, \Gamma_8^+)] - [E_{\text{gap}} + E(2\Gamma_1, \Gamma_5, \Gamma_8^+) - E(\Gamma_1\Gamma_5, \Gamma_8^+)] \\ &= E(\Gamma_1\Gamma_5, \Gamma_8^+) - E(2\Gamma_1, \Gamma_8^+) . \end{aligned}$$

In the most extreme case, that of arsenic in silicon, the calculated value of Δ_1 is 11.32 meV, while the experimental value is only 5.4 meV. One consequence of overestimating the electron excitation energy is to underestimate the binding energies of larger complexes, since for $M > 1$ ground states include electrons in Γ_5 orbitals.

If we define an exciton binding energy

$$\begin{aligned} W_M &= E_{\text{ground}}(M-1) + E_{\text{exciton}} \\ &\quad - E_{\text{ground}}(M) , \end{aligned} \quad (27)$$

we obtain the energy gained when a free exciton combines with a complex of size $M-1$ to produce a complex of size M . The energy of a free exciton relative to a free electron and a free hole is -4.18

meV for germanium and -14.71 meV for silicon. In order for the formation of a complex of size M to be likely at a temperature T , W_M must be positive and considerably greater than kT .

We list predicted values of W_M in Table VII, with values obtained from experimental data in parentheses. Agreement is excellent for impurities in Ge and satisfactory for Si, with the notable exception of As:Si. For this system, the extremely large calculated value for the electron excitation energy of a BMEC attached to arsenic in silicon actually generates a large negative value of W_2 . If W_2 really had this value, there would be no BMEC's of size greater than $M=1$ attached to arsenic, and of all the β series and α series, only α_1 would be observed. In fact lines as high in the

series as α_6 have been seen.⁴

In germanium, on the other hand, the experimental evidence indicates that complexes of size $M > 1$ are rare. The experimental and theoretical values of W_2 are all less than or equal to 0.75 meV, which corresponds to a temperature of 9 K, while the spectra were obtained at a temperature of 5 K,^{6,7} which was high enough to dissociate most BMEC's of size $M = 2$. An experimental α_2 line was observed, but it was weaker than all the other lines including the forbidden $\alpha_1\Gamma_5$ line.

A feature of the experimental spectra which our theory does not attempt to reproduce is the fourfold splitting of the γ_1 , δ , and α_2 lines in germanium, which is due to a fourfold splitting of the $M = 1$ electron excited state ($\Gamma_1\Gamma_5, \Gamma_8^+$). This is, in turn, probably a term splitting caused by interaction between the Γ_5 electron and Γ_8^+ hole: $\Gamma_5 \times \Gamma_8 \rightarrow 2\Gamma_8 + \Gamma_6 + \Gamma_7$. The term splitting in silicon seems to be too small to detect. Our predicted positions for the α_2 , γ_1 , and δ lines for phosphorus in germanium all lie within the range covered by the fourfold experimental lines.

Our theory predicts the position of recombination lines in germanium, as well as α -series lines in silicon, with great success. The theory's chief defect is that it overestimates electron excitation energies, consequently underestimating binding energies of complexes and leading to relatively less accurate positions of the β lines. The larger the donor excitation energy, the worse the error. The theory accurately predicts that BMEC's of size $M > 1$ in germanium will be rare at all but extremely low temperatures.

VI. ALTERNATE METHODS OF CALCULATING BMEC ENERGIES

The results reported in the previous section are more or less sensitive to the approximations

TABLE VII. Theoretical and experimental exciton capture energies W_M for BMEC of size M , for several donor species. The experimental values are given in parentheses with the source indicated by a superscript. Experimental values are obtained by subtracting the free-exciton position (1154.59 meV for silicon and 740.46 meV for germanium) from α_1 for $M = 1$, β_{M-1} for $2 \leq M \leq 4$, and β'_{M-1} for $M > 4$.

M	W_M (meV)					
	P,Bi:Ge	As:Ge	P:Si	Sb:Si	As:Si	
1	1.52(1.25) ⁶	1.80(1.39) ⁶	5.11(4.58) ¹	4.47(4.5) ⁴	4.65(5.4) ⁴	
2	0.52(0.75) ⁶	0.37(0.62) ⁶	1.61(4.0) ²	1.54	-3.43(3.2) ⁴	
3	1.35	1.25	4.45(6.69) ¹	5.03(7.2) ⁴	3.00(8.3) ⁴	
4	2.05	1.91	6.75(8.99) ¹	7.20(9.5) ⁴	3.71(10.0) ⁴	
5	1.85	1.76	5.37	5.30	2.50	
6	2.29	2.18	6.78(9.8) ²	6.75	5.50	

described in Sec. IV. In order to display the dependence on these approximations, and to examine their significance, we have tested several other methods of combining band-structure effects with density-functional theory to calculate the energies of BMEC's. The two main variations of the density-functional method which we consider are self-interaction corrections, used in calculations D through F below, and the spin-density-functional method, which calculations G and H employ. We describe calculations A through H in order below, as well as giving reasons for their use.

First, we describe calculations which test the sensitivity of our method of treating the conduction-band valley-orbit splitting (Sec. IV A) to the cutoff factor α defined in Eq. (18). In these calculations, we use the ordinary non-spin-dependent density-functional method, but allow the conduction-band \vec{k} -space position vector $\vec{\eta}$ (defined so that $\vec{k} = \vec{G} + \vec{K}_i + \vec{\eta}$, with \vec{G} being a reciprocal-lattice vector and \vec{K}_i the i th equivalent minimum of the conduction band) to range over different volumes of \vec{k} space.

Method A is the basic method of this paper, as described in Sec. IV. If the conduction band has N equivalent minima, the vector $\vec{\eta}$ ranges over $1/N$ of the volume of a Brillouin zone.

Method B allows $\vec{\eta}$ to range over $2/N$ the volume of a zone. We do this to approximate the two-band theory of Pantelides,³⁵ based on the observation that the valleys in the conduction band of silicon are near the edge of the Brillouin zone. Thus the energies and momenta of particles in the adjoining part of the next-higher band are closer to the valley minimum than are the energies and momenta of particles in the conduction band near the center of the zone. It is therefore important to include both bands in calculations of donor states.

Method C allows $\vec{\eta}$ to range over all \vec{k} space,

which is equivalent to including an infinite number of bands in the calculation. This was the method used in Refs. 28 and 29. Method C yields BMEC energies which are close to those produced by method A, although the depth V_0 of the central-cell correction is much smaller. This implies that, when using ordinary density-functional theory, if one produces similar donor energies by different methods, one will also obtain similar BMEC energies. As one might expect, the results of method B consistently fall between the results of methods A and C.

Zunger *et al.*³⁶ have used a self-interaction-corrected (SIC) density-functional method³⁷ to calculate energies of atomic states with great accuracy. The SIC method reduces errors in energies of atomic states calculated by the ordinary density-functional method. The overestimate of the electron excitation energy which methods A through C produce declines as the complexes increase in size, so that it may be reasonable to assign the error to the inclusion of interactions of particles with themselves. The SIC method tested here differs somewhat from that of Ref. 37, since we are applying the correction to a non-spin-dependent energy functional. Thus, method D is identical to method A, except that all of the self-interaction contributions to the energy are subtracted out.

Method E omits the electron exchange energy term of the exchange-correlation energy. Since the electrons in a small BMEC are all in $1s$ orbitals in different spin states or different valleys, the actual exchange energy should be negligible. Thus, the use of an exchange term derived from a uniform electron-hole liquid is suspect. The calculation of method E is performed in order to test whether the exchange term is in fact needed to obtain satisfactory agreement with experiment.

Method F is an SIC calculation as in method D, but $\vec{\eta}$ is allowed to range over all \vec{k} space, as in method C.

The second main variation of the density-functional method is the spin-density-functional method,³⁸ which treats the total energy as a functional of spin-up electron density $\rho_{e\uparrow}$, spin-down electron density $\rho_{e\downarrow}$, and hole density ρ_h . A spin-dependent energy functional will result in different energies for $\Gamma_{1\uparrow}\Gamma_{5\uparrow}$ and $\Gamma_{1\downarrow}\Gamma_{5\downarrow}$ electron configurations. For this calculation, only the exchange part of E_{xc} is spin dependent; i.e., the $\rho_e^{1/3}$ term of Eq. (6) is split into separate spin-up and spin-down parts. One goal of this calculation, method G, is to determine, as in method E, whether the electron

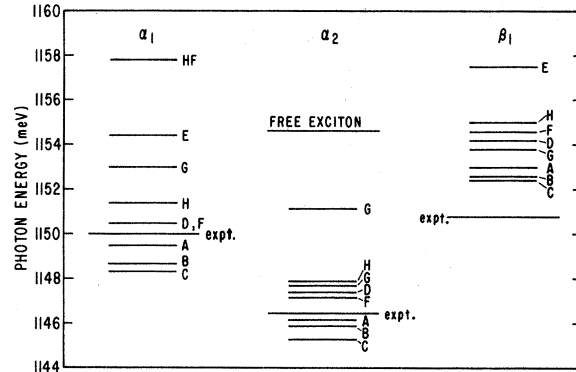


FIG. 4. Positions of recombination lines α_1 , α_2 , and β_1 predicted by calculations described in Sec. VI. Also included is the predicted position of α_1 obtained by the Hartree-Fock method (Ref. 15). The positions are given in meV.

exchange term of Eq. (6) corresponds to a genuine exchange interaction.

Method H employs an SIC spin-density-functional calculation and is the method which estimates atomic energies most accurately.

We have used all of these methods to calculate the energies of BMEC's of size $M \leq 2$ attached to phosphorus in silicon. Figure 4 gives the resulting positions of the α_1 , α_2 , and β_1 lines for each of these methods, as well as the α_1 position predicted by the Hartree-Fock method.¹⁵ Method G produces two α_2 lines because the $\Gamma_{1\uparrow}\Gamma_{5\uparrow}$ and $\Gamma_{1\downarrow}\Gamma_{5\downarrow}$ states have different energies.

The best fit to experimental data is produced by method A, the primary method of this paper. The inclusion of "extra bands" (methods B and C) changes the predicted positions of recombination lines only slightly, with the calculated β_1 line moving toward the experimental value and the α lines moving away.

Self-interaction correction actually increases the overestimation of the electron excitation energy. Both methods D and F do not significantly improve agreement between the experimental and theoretical position of α lines, and predict a position for β_1 corresponding to a binding W_2 of less than 1 meV.

If we leave out the electron exchange term (method E), the $M = 1$ complex is barely bound ($W_1 = 0.18$ meV) and the $M = 2$ complex is strongly unbound ($W_2 = -2.90$ meV). This indicates that the electron exchange term of Eq. (6) is needed to produce bound complexes.

The spin-density-functional method (methods G and H) predicts recombination line positions which

differ from their experimental values by amounts exceeding the experimental electron excitation energy. This result is a consequence of the strong spin dependence of the electron exchange energy in this calculation.

Thus, of the methods described in this section, method A, the single-band density-functional theory of Sec. IV, gives the best agreement with experiment. The implications to be drawn from this result will be discussed in the next section.

VII. DISCUSSION

From the preceding section, we find that of the methods tested the best agreement between theory and experiment is obtained using a simple non-spin-dependent density-functional method without self-interaction correction, with an exchange-correlation energy obtained from the uniform electron-hole liquid. Further, unlike the situation for ordinary atoms, the inclusion of exchange-correlation energy is essential to obtain binding at all.

There are two fundamental questions raised by the success of method A of Sec. VI. The first concerns the successful use of a spin-independent E_{xc} . For a multivalley semiconductor with N valleys, the actual electron exchange energy should be negligible for any BMEC containing $2N$ or fewer electrons in the ground state, since there is no exchange between electrons of different spin and very little between electrons in different valleys. Nevertheless, it is necessary to include the electron exchange term derived from the uniform electron gas in the energy functional in order to obtain bound states. Furthermore, when, in employing spin-density-functional theory (methods G and H in Fig. 4), we treat the exchange term as if it represented the exchange interaction between electrons in separate single-particle orbitals, we obtain inaccurate estimates of BMEC energies. The density-functional theory of Secs. II and IV treats the exchange terms in Eq. (6) in precisely the same manner as the correlation terms.

Our interpretation of these results is that the local energy functional of Eq. (6) remains reasonably valid for systems with a small number of particles only if we abandon the separate identification of the $\rho^{1/3}$ and $\rho^{1/6}$ terms with exchange and correlation energy, respectively. Further, in this case of a multivalley semiconductor, an attempt to construct a spin-dependent extension of Eq. (6) does *not* pro-

duce a useful local energy functional for small systems. A possible cause of this behavior of ϵ_{xc} is as follows. With less than one electron of given spin direction in a given valley, there is no electron exchange and hence no exchange hole keeping electrons of like spin apart. Under these conditions, the magnitude of correlation energy will increase due to an enhanced correlation hole. Hence, the sum of exchange plus correlation may be much less sensitive to the number of particles than each component, as least for the range of densities considered here. Since ϵ_{xc} would then be essentially all correlation energy, we would expect the spin dependence to be very weak.

The second point that requires comment concerns the fact that, unlike the case for atoms, correlation energy is a major component of the total energy in these systems.

This situation brings the validity of the shell model, with its single-particle orbitals, into question. If the electrons and holes truly existed in independent single-particle orbitals (i.e., if a single Slater determinant was a good approximation to the wave function), then the Hartree-Fock method, as used in Ref. 15, should give a reasonably good estimate of the ground-state energy of a bound exciton ($M=1$). However, the Hartree-Fock ground-state energy of -57 meV for a bound exciton attached to phosphorus in silicon is about 7 meV higher than the experimentally derived ground-state energy, and about 8 meV higher than our estimate of the energy. Furthermore, the Hartree-Fock estimate of the bound-exciton ground-state energy is 3 meV higher than the combined energy of a donor and a free exciton (-60 meV), which implies that without correlation energy, excitons would not attach themselves to donors and no BMEC's of any size would form. Thus, the actual wave function must contain strong correlations between the positions of the particles, so that the "single-particle" orbitals of the shell model cannot be interpreted literally.

This problem is quite distinct from the problems of a multivalley semiconductor. To investigate this question, we look at the model system "positronium-hydride," consisting of a fixed positive charge, two electrons, and one positron. In most studies of this model, the ratio of the electron and positron mass, $\sigma = m_e/m_h$, is regarded as an input parameter to an energy calculation. Stebe and Munsch³⁹ have performed variational calculations on a parameterized many-body wave function of this system and obtained the energy as a function of σ .

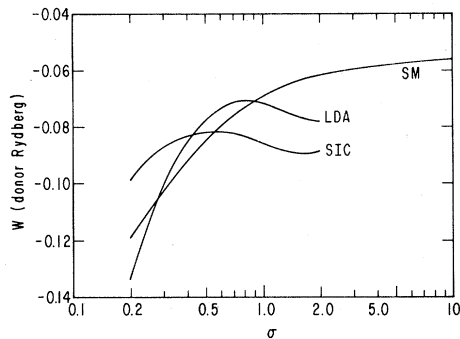


FIG. 5. Binding energy $W = E - E_{\text{donor}} - E_{\text{exciton}}$ of a single exciton to a donor as a function of the ratio of electron and hole masses $\sigma = m_e/m_h$, ($1 \text{ Ry} = \frac{1}{2} m_e e^4 / \hbar^2$). LDA represents a local density-functional calculation (Ref. 40), SIC a self-interaction-corrected calculation, and SM a calculation employing a completely parametrized three-body wave function (Ref. 39).

Wünsche and Henneberger⁴⁰ have done a density-functional calculation, including exchange and correlation terms, which agrees well with the results of Ref. 39. We have reproduced the calculations of Ref. 40 and have also performed self-interaction-corrected and Hartree-Fock calculations for this model problem. In Fig. 5 we display the binding energy $W = E_{\text{total}} - E_{\text{donor}} - E_{\text{xc}}$ as a function of σ in units of the donor Rydbergs ($1 \text{ Ry} = m_e e^4 / 2 \hbar^2$) for the three methods. Hartree-Fock energies are unbound and off scale in Fig. 5; typical values are $W = +0.25 \text{ Ry}$ for $\sigma = 0.5$,

$W = +0.17$ for $\sigma = 1.0$, $W = +0.10 \text{ Ry}$ for $\sigma = 2.0$. Again the density-functional method without self-interaction correction produces a remarkably good approximation to the "exact" results of Ref. 39.

We are left with the problem of interpreting the single-particle orbitals produced by the density-functional method. We can suppose that, as in any density-functional calculation, the wave functions are simply an intermediate construct used to obtain the kinetic energy and the density, to which no special significance should be attached. This point of view can be maintained if we are concerned only with the shell-model energies. Yet the shell-model selection rules predict all the major series' of recombination lines, with the minor exception of the weak "forbidden" $\alpha_1 \Gamma_5$ line in germanium. The single-particle character of the selection rules implies that the wave functions have significance beyond simply being artifacts of the density-functional method. There is thus a need for a physical explanation for the success of the single-particle shell model in a system in which correlation energy plays a major role, perhaps an explanation involving a quasiparticle interpretation of the single-particle-like wave functions of density-functional theory.

ACKNOWLEDGMENTS

This work was supported by the National Science Foundation under Grant No. DMR 79-20813.

¹M. L. W. Thewalt, *Can. J. Phys.* **55**, 1463 (1977).

²M. L. W. Thewalt, *Proceedings of the Fifteenth International Conference on the Physics of Semiconductors, Kyoto, 1980* [*J. Phys. Soc. Jpn.* **49**, Suppl. A, 437 (1980)].

³A. S. Kaminskii, V. A. Karasyuk, and Ya. E. Pokrovskii, *Zh. Eksp. Teor. Fiz.* **74**, 2234 (1978) [*Sov. Phys.—JETP* **47**, 1162 (1978)].

⁴K. R. Elliott and T. C. McGill, *Solid State Commun.* **28**, 491 (1978).

⁵R. W. Martin, *Solid State Commun.* **14**, 369 (1979).

⁶A. E. Mayer and E. C. Lightowers, *J. Phys. C* **12**, L539 (1979); **12**, L945 (1979).

⁷A. E. Mayer and E. C. Lightowers, *J. Phys. C* **13**, L747 (1980).

⁸G. Kirzenow, *Solid State Commun.* **21**, 713 (1977); *Can. J. Phys.* **55**, 1787 (1977).

⁹P. Hohenberg and W. Kohn, *Phys. Rev.* **136**, B804 (1964).

¹⁰W. Kohn and L. J. Sham, *Phys. Rev.* **140**, A1133 (1965).

¹¹H. B. Shore and R. S. Pfeiffer, in *Proceedings of the Fourteenth International Conference on the Physics of Semiconductors, Edinburgh, 1978*, edited by B. L. H. Wilson (The Institute of Physics, Bristol, 1978), p. 627.

¹²J. H. Rose, L. M. Sander, H. B. Shore, and R. S. Pfeiffer, *Solid State Commun.* **29**, 389 (1979); **30**, 697 (1979).

¹³J. H. Rose, private communication.

¹⁴H.-J. Wünsche, K. Henneberger, and V. E. Khartsiev, *Phys. Status Solidi B* **86**, 505 (1978).

¹⁵Y. C. Chang and T. C. McGill, *Phys. Rev. Lett.* **45**, 471 (1980).

¹⁶W. F. Brinkman and T. M. Rice, *Phys. Rev. B* **7**, 1508 (1973).

¹⁷J. H. Rose and H. B. Shore, *Phys. Rev. B* **17**, 1884 (1978).

- ¹⁸R. K. Kalia and P. Vashishta, *Phys. Rev. B* **17**, 2655 (1978).
- ¹⁹J. H. Rose, private communication.
- ²⁰L. M. Sander, H. B. Shore, and J. H. Rose, *Solid State Commun.* **27**, 331 (1978).
- ²¹T. L. Reinecke and S. C. Ying, *Phys. Rev. Lett.* **35**, 311 (1975).
- ²²V. S. Bagaev, N. N. Sibel'din, and V. A. Tsvetkova, *Zh. Exp. Teor. Fiz. Pis. Red.* **21**, 180 (1975) [*JETP Lett.* **21**, 80 (1975)].
- ²³J. Collet, M. Pugnet, J. Barrau, M. Brousseau, and H. Maanef, *Solid State Commun.* **24**, 335 (1977).
- ²⁴L. Resca and R. Resta, *Solid State Commun.* **29**, 279 (1979), and references therein.
- ²⁵R. Resta, L. Resca, and H. B. Shore, *Phys. Rev. B* **25**, 4031 (1982).
- ²⁶A. Baldereschi and N. O. Lipari, *Phys. Rev. B* **8**, 2697 (1973).
- ²⁷K. S. Mendelson and H. M. James, *J. Phys. Chem. Solids.* **25**, 729 (1964).
- ²⁸H. B. Shore and R. S. Pfeiffer, Proceedings of the International Conference on the Physics of Semiconductors, Kyoto, 1980 [*J. Phys. Soc. Jpn.* **49**, Suppl. A, 453 (1980)].
- ²⁹R. S. Pfeiffer and H. B. Shore, *Solid State Commun.* **40**, 165 (1981).
- ³⁰A. Onton, P. Fisher, and A. K. Ramdas, *Phys. Rev.* **163**, 686 (1967).
- ³¹R. L. Jones and P. Fisher, *J. Phys. Chem. Solids* **26**, 1125 (1965).
- ³²J. H. Reuszer and P. Fisher, *Phys. Rev.* **135**, A1125 (1964).
- ³³R. L. Aggarwal and A. K. Ramdas, *Phys. Rev.* **140**, A1246 (1965).
- ³⁴P. K. W. Vinsome and D. Richardson, *J. Phys C* **4**, 2650 (1971).
- ³⁵S. T. Pantelides, *Solid State Commun.* **30**, 65 (1979).
- ³⁶A. Zunger, J. P. Perdew, and G. C. Oliver, *Solid State Commun.* **34**, 933 (1980).
- ³⁷J. P. Perdew and A. Zunger, *Phys. Rev. B* **23**, 5048 (1981).
- ³⁸O. Gunnarsson and B. I. Lundquist, *Phys. Rev. B* **13**, 4274 (1976).
- ³⁹B. Stebe and G. Munsch, *Solid State Commun.* **35**, 557 (1980).
- ⁴⁰H.-J. Wünsche and K. Henneberger, *Phys. Status Solidi B* **91**, 331 (1979).